

## EFFECT OF LOCAL MISTUNING OF BLADE VIBRATION FREQUENCIES ON THE VIBRATION STRESS OF COMPRESSOR AND TURBINE DISKS OF AIRCRAFT GAS TURBINE ENGINES

A. P. Zinkovskiy,\* K. V. Savchenko,<sup>1</sup> O. L. Derkach,  
and I. G. Tokar

UDC 543.1:62-226

*The effect of engineering and process factors on the vibration stress of the cantilevered bladed disks of the 1st stage – low-pressure compressor and the shrouded blades of the 2nd stage – free power turbine for different types of aircraft gas turbine engines is investigated. The results of calculation-experimental studies on the frequency mistuning effect caused by the reduction of the cantilevered blade face length and its transition thinning to the shroud platform on the vibration stress of the intergroove ribs of the disk and blade rings, respectively, are presented. Three-dimensional finite element models of disks with the break of cyclic symmetry due to the vibration frequency mistuning of one blade, as the most dangerous case of the natural frequency scattering over the blade rings, were constructed. Calculation and experimental studies on the vibration stress of the intergroove ribs were carried out for two disk modifications with different rim thicknesses. The results of the complex calculation studies demonstrated that the resonant vibration amplitudes were localized in the vicinity of the frequency-mistuned blade. Thus, in the vicinity of the blades with the cross-section thinning of their face, the difference in the distribution of maximum equivalent stress zones is observed, which can lead to the localization of blade vibrations with their further failure. At the same time, the vibration stress of the intergroove ribs is established to depend on the vibration excitation harmonic, as well as the elastic bladed disk connection, which is determined by its stiffness. The results of computational experiments suggestive of reducing both the vibration stress and the localization level of resonant vibration amplitudes by analyzing and establishing those characteristics that effect the connection stiffness, which is of great practical importance for improving the vibration reliability of aircraft engine disks.*

**Keywords:** bladed disk, mistuning of blade vibration frequencies, frequency function, vibration stress, intergroove rib, shrouded blades.

**Introduction and Statement of the Problem.** Reliable operation and service life of aircraft gas turbine engines (GTE) are one of the major challenges based on prediction of possible failures of the bladed disks of the compressor and turbine due to their heightened vibration stresses caused mainly by wide-range dynamic loads.

Calculation and experimental studies demonstrate that the scatter of engineering and process parameters of blade rings can significantly affect their vibration stress. This is due to the difference in the blade geometry, such as the size of the blade face cross-section and its length, which effects the ratio of their elastic and inertial characteristics. Therefore, the blade ring asymmetry can be integrally characterized by the vibration frequency mistuning of single

---

\* Deceased.

---

Pisarenko Institute of Problems of Strength, National Academy of Sciences of Ukraine, Kyiv, Ukraine (savchenko@ipp.kiev.ua). Translated from Problemy Mitsnosti, No. 1, pp. 18 – 32, January – February, 2023. Original article submitted October 4, 2022

blades. Moreover, the blade incidence may vary, slightly differ in the surface shapes, etc. In this case, critical blade ring operation modes can happen, which featuring the splitting of paired vibration frequencies [1, 2], distortion of sinusoidal vibration modes [3, 4], and modal localization and scattering of resonant vibration amplitudes [5–8].

At the same time, previously performed experimental and computational studies [10–13] to establish possible reasons for the failure of intergroove ribs in the compressor disks of several aircraft GTE showed that their stress was strongly dependent on the disk rim thickness, blade vibration modes, and their inevitable mistuning, which would require further research to reveal the sources of crack origin and possible failures of intergroove ribs [9, 10]. Thus, experimental data [11] for the 1st stage-low-pressure compressor (LPC) of an aircraft GTE with a dovetail-joined cantilevered bladed disk disclosed the crack initiation from the sharp angle of the intergroove rib and the dynamic blade stress effect on its vibration stress. These conclusions were indirectly confirmed by computational results obtained for rod models [12]. The three-dimensional models of the above disk [13] take into complete account its geometry, material properties, boundary conditions, and active loads. They were used to investigate the effect of centrifugal forces on the stress state of the intergroove ribs in the two disk modifications with different rim thicknesses. Thus, the experimental data [11] were confirmed, and it was shown that the compressor disk rim thickening by 1.36 times resulted in a decrease in maximum static stresses near the acute angle vertices by approximately 10%. The vibration stress of the intergroove ribs was found to remain high, ranging from 20 to 30% of the blades vibration stress level.

For analyzing the system vibrations at the break of symmetry, there is a need to examine not one of its periods but the system as a whole. This significantly complicates the problem compared to cyclically symmetric systems for which the examination of the blade rings as a whole is replaced by the analysis of a single cycle period with appropriate boundary conditions [14]. Since the problem was quite complicated and the capabilities of computing tools were limited, at the initial stage of research, discrete models have gained wider acceptance. Such models, despite their simplicity, could determine the basic symmetry break mechanism giving rise to the system vibrations. Thus, in particular, they permitted of establishing the localization mechanisms of vibrations for the systems with disrupted regularity of single-type subsystems, revealed, possible reasons for the increased vibration stress of blade rings, and provided recommendations for its reduction [12–14]. However, the stress state can be investigated in detail only on the basis of a continual or three-dimensional finite element (FE) model, which should take account of the dynamic properties of single-type and mistuned blades of complex geometry, as well as their interaction through disk or shroud elements.

The object of the study is the calculation-experimental investigation based on three-dimensional FE models to establish the effect of the vibration frequency mistuning of one blade, as the most dangerous case of the natural frequency scattering over LPC and free power turbine (FPT) bladed disks of aircraft GTE, caused by engineering and process factors, on the vibration stress of the intergroove ribs and substantiation of the blade vibration frequency mistuning as a possible source of in-service disk failure.

**Research Objects and Simulation.** The bladed disks of the 1st stage LPC of turbofan and the 2nd stage FPT of turboshaft aircraft GTE, with 35 and 51 blades ( $N = 35$  and  $51$ ) were chosen as the objects of investigation.

The LPC does not have shroud platforms between the blades using the dovetail disk joint with flat surfaces. The study was conducted for two disk modifications with different rim thicknesses  $l$ :  $1 - l_1 = 22$  mm and  $2 - l_2 = 30$  mm. The disk and blades are made of a titanium alloy with the following physicomechanical characteristics: Young's modulus  $E = 115$  GPa, density  $\rho = 4500$  kg/m<sup>3</sup>, and Poisson's ratio  $\mu = 0.3$ .

The FPT disk blades possess Z-shroud platforms. The two versions of blade rings were examined: 1 – the geometry of the blade faces corresponds to the design documentation; 2 – the blades exhibit the face cross-section thinning to 0.27 mm at the trailing and to 0.35 mm at the leading edges. The blades are made of a heat-resistant nickel alloy with the following physicomechanical characteristics: Young's modulus  $E = 190$  GPa, density  $\rho = 8570$  kg/m<sup>3</sup>, and Poisson's ratio  $\mu = 0.3$ .

The complexity of the disk design would require reliable analysis of the stress state based on three-dimensional simulation. The models of LPC disks and FPT blade rings were constructed using three-dimensional quadratic finite element and its modifications. The basic principles of constructing the FE blade models are given in [15]. The FE models of the LPC disk of modification 1 and the FPT disk sector with the shrouded blade are shown in Fig. 1.

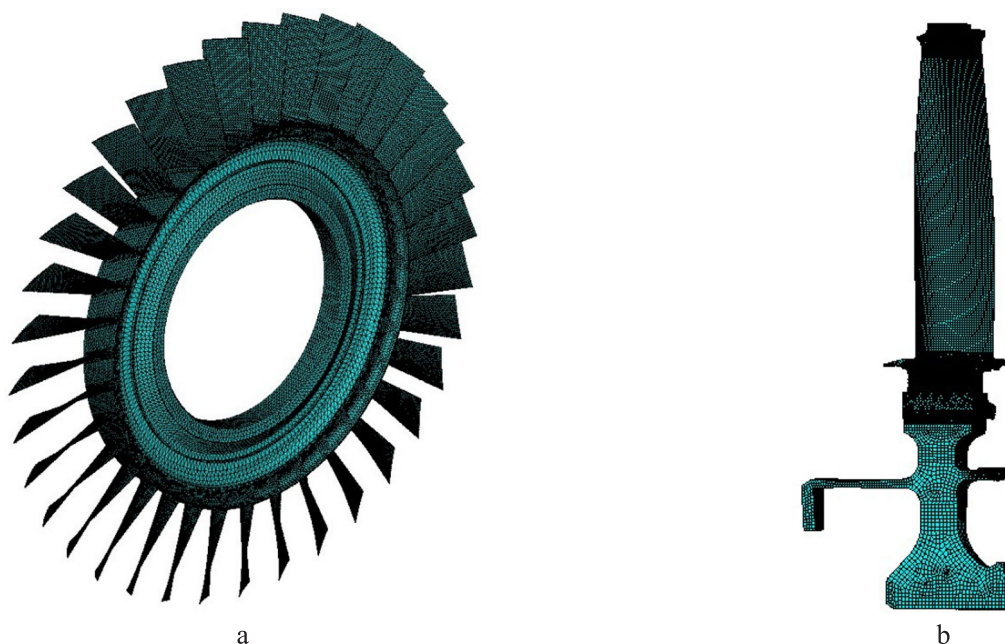


Fig. 1. FE model of the aircraft GTE LPC disk of modification 1 (a) and FPT disk cycle period (b).

In computational studies on the LPC disks, the stiff disk-blade connection over the contact root surfaces was assumed, which is characteristic of engine service conditions. At the same time, the totality of computational experience shows that the blade vibration frequency mistuning is not influenced by the operating engine mode [16]. The reliability of the compressor models is confirmed in [13] where the calculation results for the vibration stress of the intergroove ribs in the disks of both modifications acted by centrifugal forces agree well with the experimental data.

For comparing the calculated disk vibration stresses with the experimental data (procedure is described in [11]), the construction of FE models took account of the arrangement of strain gauges on the intergroove ribs (Fig. 2). The FE model construction of the LPC disk included the arrangement of strain gauges in the corresponding points on the platforms of its grooves, as shown in Fig. 2: six (Nos. 1–3 on the right and Nos. 4–6 on the left) across the width ( $h$ ) of the groove in the joining zone of its inclined plane with the cylindrical rim surface and four at the disk end (Nos. 7, 9 from the leading and Nos. 8, 10 from the trailing blade face edges).

For the LPC disks of modifications 1 and 2 and the FPT disk of version 1 exhibiting structural cyclosymmetry, the evaluation of vibration characteristics is reduced to the examination of a single period with the corresponding boundary conditions. As a rule, the disk period is its sector with one blade, and the order of cyclosymmetry coincides with the number of blades  $N$ .

For establishing the principles of the natural vibration frequency spectrum formation of the research object, the exclusion of any nonlinear interaction of the system elements is of decisive importance. Therefore, for simulating the contact blade-FPT disk interaction, the displacement compatibility conditions were imposed on all nodes of finite elements of the contact joint surfaces. Moreover, the models of the period were rigidly fixed over the disk interior, simulating its operation as a part of the FPT rotor.

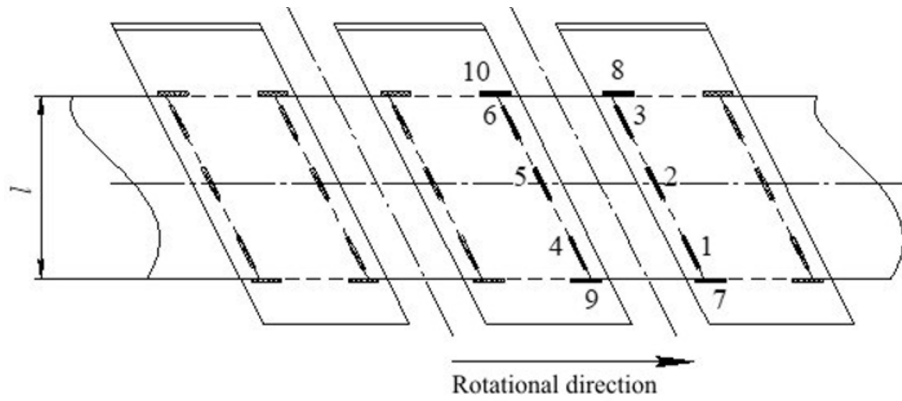


Fig. 2. Scheme of strain gauge arrangement across the width of the intergroove ribs (Nos. 1–6) and on the end surface (Nos. 7–10) of the 1st stage LPC disk rim.

The contact interaction of the shroud platforms of FPT blades was simulated after the results of solving the static problem with a given field of centrifugal forces and temperature gradient with determining their contact zones. This problem was solved using the surface–surface contact elements after a procedure [17]. Furthermore, between the FE nodes of the contact surfaces wherein nonzero contact pressures exist, spring elements with one degree of freedom are generated, which were arranged along two mutually orthogonal axes to the contact plane of shroud platforms. Each element is given the pressure values that were determined in the corresponding nodes of solving the static problem. On the nodes with maximum contact pressures, the displacement compatibility conditions in the radial direction (along the blade face) are additionally imposed. Such linearization of the contact interaction of shroud platforms can ensure a more realistic assessment of the system stiffness and, accordingly, natural vibration frequencies in comparison with the rigid fixation and imposition of displacement compatibility [18].

**Results and Discussion.** The first stage of the study included the use of the FE models in computational experiments to determine the spectrum of natural vibration frequencies of the LPC and FPT disks their strict cyclic symmetry and its break. With this, the blade vibration frequency mistuning was employed to include the possible change in the blade face geometry both in production and GTE service.

Examine the computational results to establish the local blade frequency mistuning effect on the natural vibration frequency spectrum formation of chosen disks. The studies were performed at the  $\Delta p_{01} = (p_j/p_{01} - 1) \times 100\%$  principal bending vibration frequency  $p_j$  mistuning of one ( $j = 5$ ) blade. This distribution was chosen since it is the most dangerous in terms of the vibration stress of the system with broken rotational symmetry.

The relative values of the frequency functions  $\bar{p}_{mn} = p_{mn}/p_{01}$  for the FPT disk of versions 1 and 2, where  $p_{01}$  is the mean value of the principal vibration frequency of a set of blades, are given in Fig. 3. By the frequency function is meant the natural vibration frequencies of the system  $p_{mn}$  against the number of strain waves  $m$  (nodal diameters) of the system, where  $n$  is the frequency function number corresponding to a given number of nodal diameters  $m$ .

Data analysis shows that the density of the natural frequency vibration spectrum of the disk depends on the frequency function number. Moreover, in a certain range of nodal diameters, the frequency functions are practically parallel to the abscissa axis, which suggests the probable localization of vibrations [4]. This is especially well seen for the first frequency function at the number of nodal diameters  $m > 12$ , as well as the second, third, and fourth frequency functions at  $m < 12$ . In this case, if the symmetry of the blade rings is broken, each blade vibrates as a separate subsystem with its own dynamic characteristics. Also arising is the interference zone of the first and second frequency functions at  $m = 12$ . This phenomenon, as noted in [19], significantly effects the formation of resonant disk vibrations at the break of their cyclosymmetry. The computational results are in good agreement with conclusions given in [10]. Similar behavior is also observed in the formation of natural vibration modes of the LPC disk.

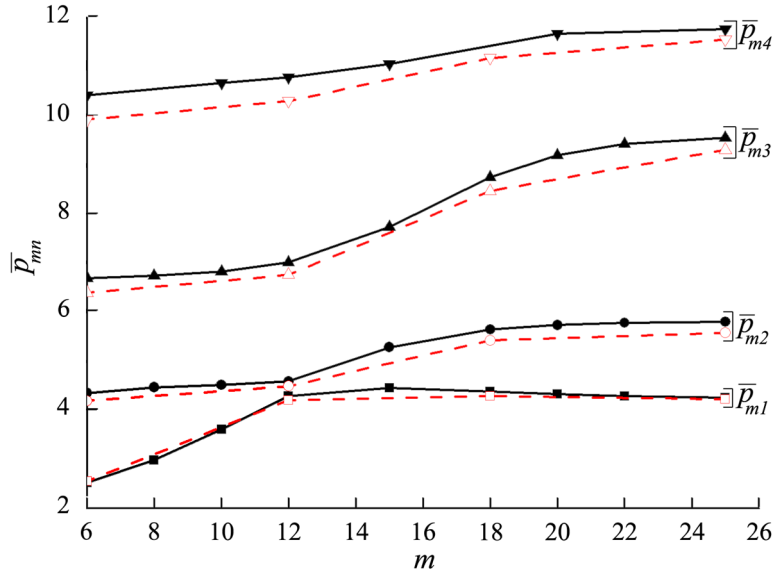


Fig. 3. Frequency functions of the FPT disk of versions 1 (solid line) and 2 (dashed line).

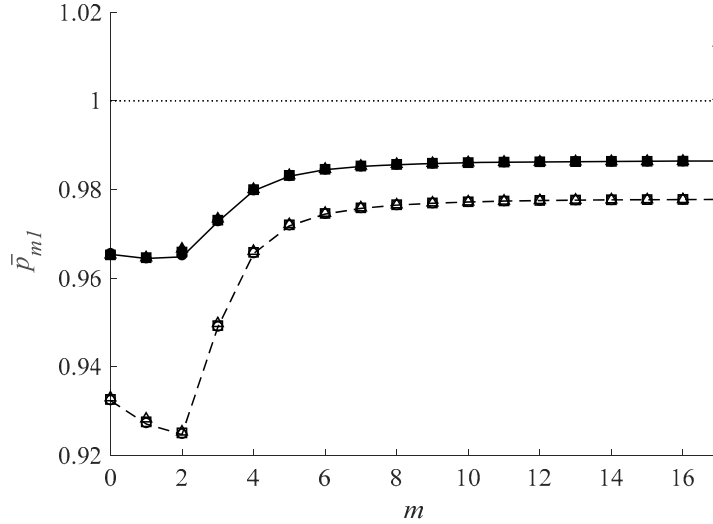


Fig. 4. Frequency functions of  $p_{m1}^{(I)}$  (lines) and  $p_{m1}^{(II)}$  (symbols) of the LPC disk on the frequency mistuning of one blade: 0.5% ( $\circ$ ,  $\bullet$ ), 1% ( $\square$ ,  $\blacksquare$ ), and 3% ( $\triangle$ ,  $\blacktriangle$ ) of modifications 1 (dashed line and open symbols) and 2 (solid line, dark symbols).

The calculation results for determining the first frequency function ( $n = 1$ ) of the natural vibration frequencies of the LPC disks of modifications 1 and 2 in the case of mistuning of the blade rings, as well as in its absence are shown in Fig. 4. The relative frequency function values confirm the conclusions based on the model of paired vibration modes [14, 20] as regards the frequency spectrum formation of the system with broken cyclosymmetry. The vibration frequency  $\Delta p_{01}$  mistuning of a single blade is due to a decrease in its face length. The studies were conducted for  $\Delta p_{01} = 0.5, 1, \text{ and } 3\%$ . Thus, when the condition  $0 < m < N/2$  is fulfilled, the frequency splitting of the paired modes  $\bar{p}_{mn}^{(I)}$  and  $\bar{p}_{mn}^{(II)}$ , i.e.,  $\bar{p}_{mn}^{(I)} \neq \bar{p}_{mn}^{(II)}$ , is taking place. For its analysis, the splitting parameter  $\Delta \bar{p}_{mn} = \left( p_{mn}^{(I)} / p_{mn}^{(II)} - 1 \right) \times 100\%$  diagrams were obtained (Fig. 5). Its highest values occur at  $m = 2$  and 17, and there is a significant “densification” of the vibration frequency spectrum of the disk of modification 2 at  $m = 2$  and 3 due to the blade vibration frequency mistuning, which may be one of the factors increasing the vibration stress of the intergroove ribs.

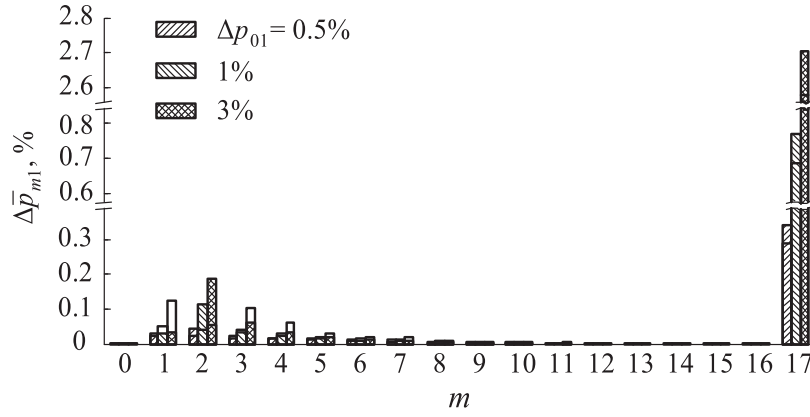


Fig. 5. Diagrams of the splitting parameter of the natural vibration frequencies of the LPC disk for modifications 1 (transparent columns) and 2 (shaded) for three values  $\Delta p_{01} = 0.5, 1,$  and  $3\%$  of the vibration frequency mistuning of one ( $j = 5$ ) blade.

Thus, the salient features of the natural vibration frequency spectrum formation are likely to significantly affect the vibration stress of the LPC disk intergroove ribs and the FPT blade rings since with the localization of the vibration modes, their stress can significantly increase. Computational studies were carried out to substantiate the conclusions as regards the probable reasons of failure caused by the localization of resonant blade vibrations. It was assumed that the blade rings were subject to the action of the driving harmonic force  $F_j = F_0 \cos[vt + (j - 1)2\pi m_{ek}/N]$ , with the amplitude  $F_0 = 10$  N and frequency  $\nu$  ( $m_{ek}$  is the designation of the  $k$ th harmonic of the driving force) applied to similar points of the face head along the axis of disk rotation.

For analysis of the resonant FPT disk vibrations, including the actual blade frequency mistuning, examine their frequency diagrams for the chosen blade geometry versions. The diagrams for the number of nodal diameters  $m = 6, 12,$  and  $25,$  defined by the engine design are presented in Fig. 6.

Their analysis demonstrates that at the excitation of FPT blade ring vibrations with the harmonic  $m_{e6},$  the resonance for their geometry version 1 comes at the excitation frequency consistent with the second natural vibration frequency of the system in the range of the rotor rotation frequency  $\omega = 1540\text{--}1600$  rad/s, which corresponds to the takeoff mode of the engine (Fig. 6a). For the FPT bladed disk of the geometry version 2, its resonant vibrations are not excited at such a rotation frequency, i.e., the blade face thinning contributes to resonance detuning-off. However, irrespective of the blade face geometry changes, as is seen from the stress intensity distribution (Fig. 7a) for both disks, the zone of their maximum values is located on the leading blade face edge in the area of its connection with the shroud platform.

At the disk vibration excitation by the driving force with the harmonic  $m_{e12}$  the resonant vibrations of blade version 1 are not excited in the ranges of rotation frequencies of service engine conditions, but for the blades of version 2, at the fourth vibration mode, the resonance is observed in the frequency range of rotor rotation  $\omega = 1695\text{--}1710$  rad/s, which corresponds to the increased rotational engine speed conditions. At such excitation parameters, as follows from the data of Fig. 7, the zone of maximum stresses for the blades of version 1 is found on the leading face edge and for those of version 2 on the trailing edge in the area of its connection with the shroud platform. In such a case, the use of the examined blades in one disk can lead to the localization of their vibrations, which is confirmed by previously obtained distributions of frequency functions for the fourth vibration mode (Fig. 3).

Under the lower power conditions of an aircraft GTE, consistent with the frequency range of  $1000\text{--}1040$  rad/s, at the excitation with the nodal diameters  $m = 25,$  the resonance of the blades of version 2 is observed at the eighth natural vibration mode. It can be excited by the harmonic  $m_{e39},$  equal to the number of blades of the 1st-stage engine compressor. However, in this case, the zone of maximum stresses is located at different heights of the leading face edge for both blade versions (Fig. 6c).

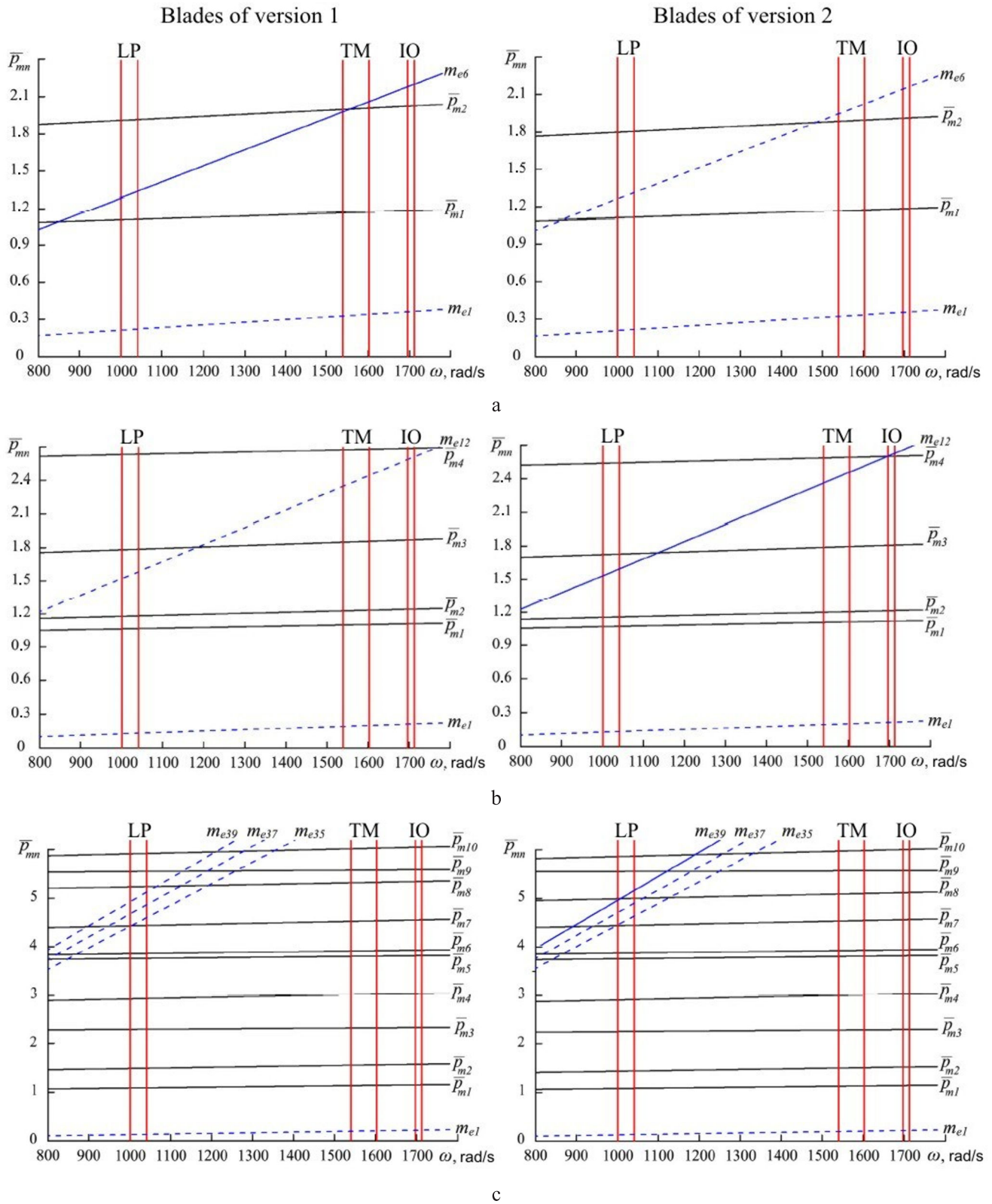


Fig. 6. Frequency diagrams of the blade rings of the 2nd stage FPT disk at the nodal diameters  $m = 6$  (a), 12 (b), and 25 (c). (LP = lower power condition; TM = takeoff mode; IO = increase operation condition.)

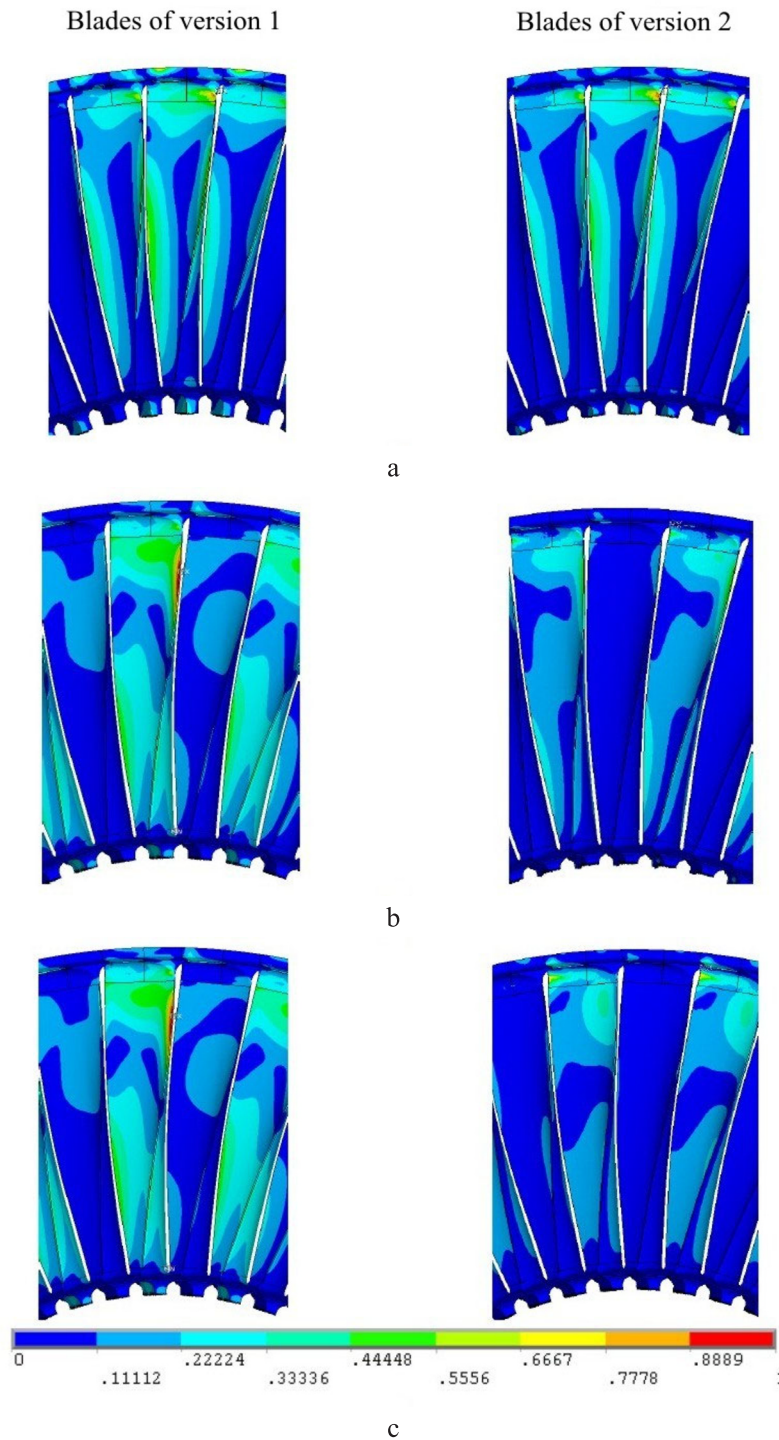


Fig. 7. Distribution of relative equivalent stresses in the FPT blade rings for versions 1 and 2 at the nodal diameters  $m = 6$  (a), 12 (b), and 25 (c).

Calculations of resonant LPC disk vibrations were carried out at the excitation of the first bending mode blade vibration with the harmonic  $m_{e3}$ , which is one of the main ones in the operation of this stage. Moreover, for establishing the general principles of resonant disk vibrations, the same calculations were performed for  $m_{e2}$ . The damping factor of the material was taken to be 0.05. For its account, the Kelvin–Feucht model was used.



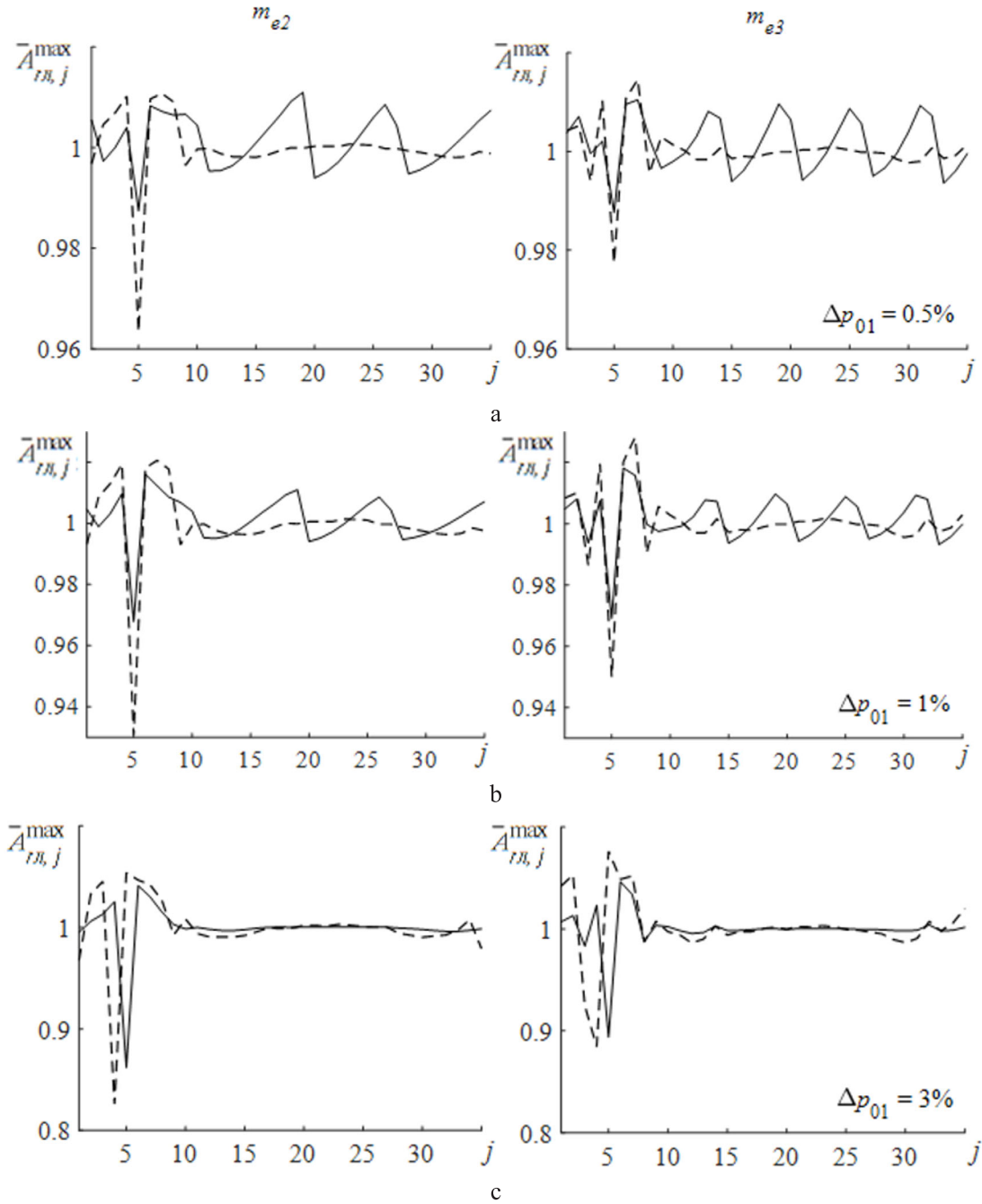


Fig. 8. Circular distribution of the relative resonant vibration amplitudes of similar points of the LPC bladed disk of modifications 1 (dashed lines) and 2 (solid lines) at the excitation by the harmonics  $m_{e2}$  and  $m_{e3}$  in the case of vibration frequency mistuning: 0.5 (a), 1 (b), and 3% (c) of one blade.

The frequency characteristics of the LPC blades were used to determine the circular distribution of maximum relative resonant vibration amplitudes in similar points of the bladed disk  $\bar{A}_{rb,j}^{max} = A_{rb,j}^{max} / A_{rb,j}^{(0)max}$ , where  $A_{rb,j}^{(0)max}$  and  $A_{rb,j}^{max}$  are the maximum resonant vibration amplitudes of the  $j$ th blade in the case of its strict symmetry and its break, respectively. The results (Fig. 8) present the following. First, the scatter of the resonant vibration amplitudes  $R = \max(A_{rb,j}^{max}) / \min(A_{rb,j}^{max})$  is greatly dependent on the excitation harmonic  $m_e$  and blade frequency mistuning, which

determine the frequency splitting of paired vibration modes and are in good agreement with the results [14, 20]. Second, for the blade with the frequency mistuning ( $j = 5$ ), the growth of the resonant vibration amplitudes is observed, which indicates their localization that is more clearly pronounced with the blade frequency mistuning level.

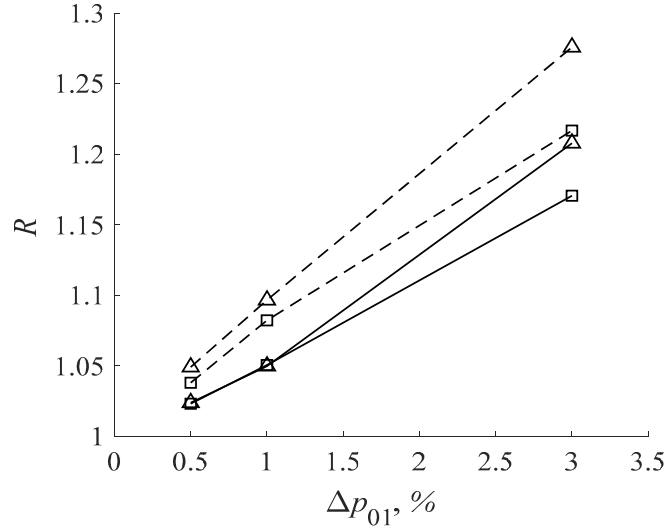


Fig. 9. Scatter of resonant vibration amplitudes of the LPC bladed disk of modifications 1 (dashed lines) and 2 (solid lines) vs the frequency mistuning of one blade at the excitation with the harmonics  $m_{e2}$  ( $\Delta$ ) and  $m_{e3}$  ( $\square$ ).

As is seen in Fig. 9, the scatter of the resonant vibration amplitudes  $R$  grows with the frequency mistuning  $\Delta p_{01}$ . With this, the disk rim thickening can reduce the scatter of resonant vibration amplitudes.

Thus, the results indicate a possibly increase in the vibration stress of the intergroove ribs of the LPC disk of both modifications at the break of symmetry due to the blade frequency mistuning. The calculations were performed to confirm the above and determine the resonant stresses in the intergroove ribs, which resulted in the circular distributions of the maximum resonant stresses  $\sigma_{rr,j}^{max}$  in the points corresponding to the strain gauge arrangement (Fig. 2) shown in Fig. 10. An increase in the resonant stress level in the intergroove ribs is of local nature and occurs in the vicinity of the mistuned blade. The most stressed is point 3 of the intergroove rib near its sharp angle. That is, the vibration stress calculations for the intergroove ribs of the LPC disk are in good agreement with the experimental results [11] as regards the initiation of fatigue cracks near the vertex of the sharp rib angle (Fig. 11).

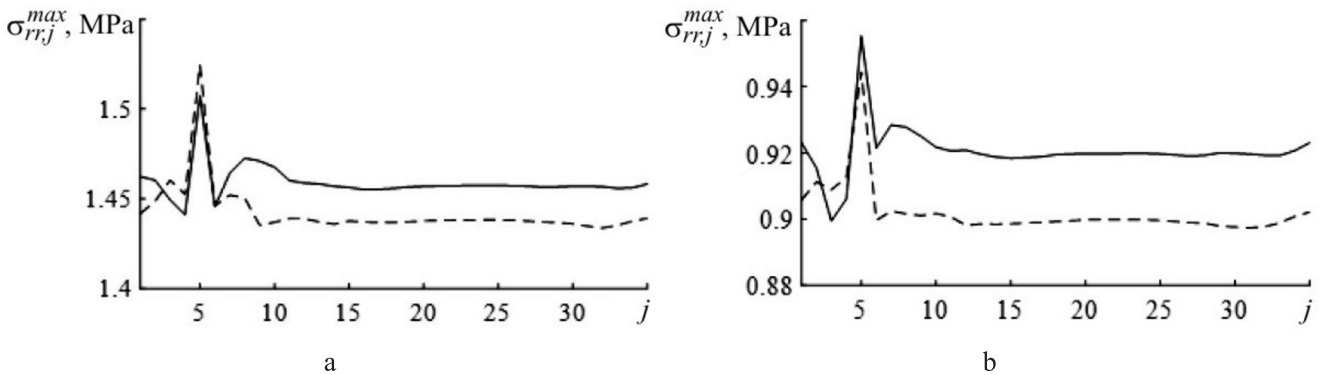


Fig. 10. Circular distribution of maximum resonant stresses of the intergroove rib of the LPC disk of modification 2 in the vicinity of the vertices of acute angles on the side of the leading (a) and trailing edges (b) of the blade at the excitation of vibrations with the harmonics  $m_{e2}$  (solid lines) and  $m_{e3}$  (dashed lines) for  $\Delta p_{01} = 1\%$ .

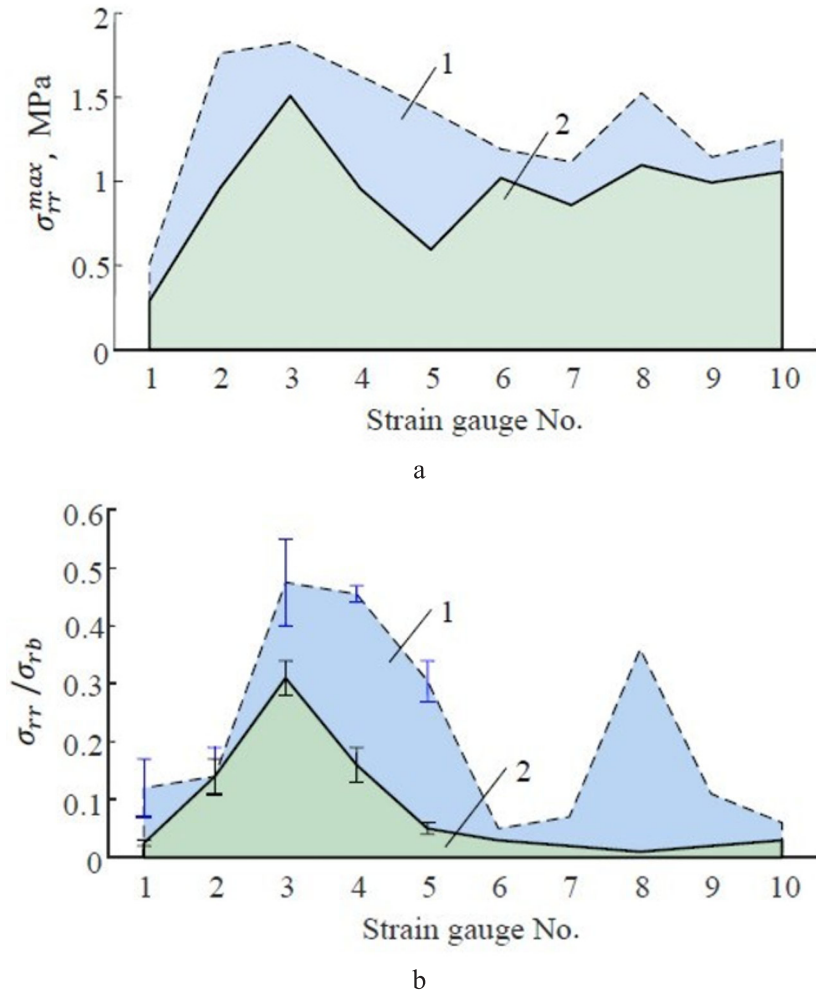


Fig. 11. Calculated distribution of the maximum vibration stresses  $\sigma_{rr}^{max}$  in the intergroove ribs of the LPC disk of modifications 1 and 2 vs 1% frequency mistuning of one blade (a) and their experimental ratio vs vibration stress  $\sigma_{rb}$  of the blade face at resonant vibrations (b).

**Conclusions.** The complex of calculation–experimental studies to determine the effect of the vibration frequency mistuning of one blade, as the most dangerous case of its distribution over the blade rings, due to engineering and process factors, on the vibration stress of aircraft GTE disks, namely, LPC with dovetail-joined cantilevered bladed disks and FPT with shrouded blades, provided the following guidelines.

1. Three-dimensional FE disk models were used to confirm the results obtained with the discrete model of blade rings, in particular, the distortion of its sinusoidal vibration modes and their localization in the vicinity of the blade with the vibration frequency mistuning.
2. The blade vibration localization level of examined systems can be determined by the frequency density of a single frequency function part of the tuned blade rings. This phenomenon in view of a probable weak modal blade connection can lead to an increase in the vibration amplitudes of such blade rings in relation to their frequency distribution.
3. The vibration stress of the intergroove ribs of the LPC disks is shown to depend on the vibration excitation harmonic, as well as on the elastic blade-disk connection defined by its stiffness. The distribution of resonant vibration amplitudes is characterized by its localization near the mistuned blade.

4. Despite an insignificant difference in the natural vibration frequencies of examined FPT blades with the face cross-section thinning, the difference in the distribution of its maximum stress zones in four vibration modes at 12 nodal diameters, can results in the localization of vibrations with further failure of some blades.

5. The results of studies on the 1st stage LPC disks of turbofan and the 2nd stage FPT of turboshaft aircraft GTE suggest the potentials of reducing both vibration stress and localization of resonant vibration amplitudes by analyzing and establishing parameters that effect the blade rigidity connection, which is of great practical importance for enhancing their vibration reliability.

## REFERENCES

1. D. J. Ewins, "The effects of detuning upon the forced vibrations of bladed disks," *J. Sound Vibr.*, **9**, No. 1, 65–79 (1969).
2. S.-T. Wei and C. Pierre, "Statistical analysis of the forced response of mistuned cyclic assemblies," *J. AIAA*, **28**, No. 5, 861–868 (1990).
3. A. P. Zin'kovskii, "Distortion of the sinusoidalness of the forms of vibrations of systems with a disturbed rotary symmetry and the mode localization phenomenon. Report 1," *Strength Mater.*, **24**, No. 10, 613–620 (1992). <https://doi.org/10.1007/BF00767878>
4. A. P. Zinkovskii, M. V. Vasil'ev, and I. N. Buslenko, "Distortion of the sinusoidalness of the forms of vibrations of systems with a disturbed rotary symmetry and the mode localization phenomenon. Report 2," *Strength Mater.*, **24**, No. 11, 678–684 (1992). <https://doi.org/10.1007/BF00768169>
5. S.-T. Wei and C. Pierre, "Localization phenomena in mistuned assemblies with cyclic symmetry. Part I: Free vibrations," *J. Vib. Acoust. Stress*, **110**, No. 4, 429–438 (1988).
6. S.-T. Wei, and C. Pierre, "Localization phenomena in mistuned assemblies with cyclic symmetry. Part II: Forced vibrations," *J. Vib. Acoust. Stress*, **110**, No. 4, 439–449 (1988).
7. A. P. Zin'kovskii, I. N. Buslenko, and V. V. Matveev, "Localization of vibrations of shrouded turbomachine rotor blading," *Strength Mater.*, **26**, No. 7, 519–526 (1994). <https://doi.org/10.1007/BF02208790>
8. O. O. Larin, "Forced vibrations of bladings with the random technological mistuning," in: Proc. of the ASME Turbo Expo 2010 (June 14–18, 2010, Glasgow), Glasgow (2010), pp. 667–672.
9. V. N. Shlyannikov, B. V. Il'chenko, and N. V. Stepanov, "Analysis of the stress-strain state of components of the lock joint of a compressor disk in a gas turbine engine in the three dimensional elastic statement. Report 1", *Strength Mater.*, **24**, No. 12, 716–721 (1992). <https://doi.org/10.1007/BF00768555>
10. N. V. Stepanov, V. N. Shlyannikov, V. V. Omel'chenko, and I. N. Shkanov, "Life of GTE disks with cracks," *Strength Mater.*, **20**, No. 4, 550–553 (1988). <https://doi.org/10.1007/BF01530872>
11. I. G. Tokar', A. Ya. Adamenko, A. P. Zin'kovskii, and V. V. Matveev, "Evaluation of vibration-induced stresses in teeth of rotor disks of compressors of gas-turbines engines," *Strength Mater.*, **29**, No. 6, 638–643 (1997). <https://doi.org/10.1007/BF02767616>
12. A. P. Zin'kovskii, "Numerical investigation of intercoupling vibration of a mistuned turbomachinery compressor wheel," *Strength Mater.*, **29**, No. 2, 150–158 (1997). <https://doi.org/10.1007/BF02767591>
13. A. P. Zinkovskiy, V. M. Merkulov, O. L. Derkach, et al., "Investigation of the stress state of the intergroove ribs of the compressor disk in view of the effect of centrifugal forces and the blade vibration frequency mistuning," *Aviats.-Kosm. Tekhn. Tekhnol.*, Issue 173/4, 47–54 (2021).
14. V. P. Ivanov, *Vibrations of Turbomachine Impellers* [in Russian], Mashinostroenie, Moscow (1983)
15. A. Zinkovskii, K. Savchenko, Y. Onyshchenko, et al., "Finite element model for analysis of characteristics of shrouded rotor blade vibrations," *IAPGOS*, **12**, No 4, 11–16 (2022). <https://doi.org/10.35784/iapgos.3264>
16. R. P. Pridorozhnyi, A. P. Zinkovskii, V. M. Merkulov, et al., "Calculation-and-experimental investigation on natural frequencies and oscillation modes of pairwise-shrouded cooled turbine blades," *Strength Mater.*, **51**, No. 6, 817–827 (2019). <https://doi.org/10.1007/s11223-020-00133-6>

17. K. Savchenko, A. Zinkovskii, R. Rzadkowski, et al., “An influence of shroud design parameters on the static stresses of blade assemblies,” MATEC Web of Conferences, Vol. 304, 03002 (2019). <https://doi.org/10.1051/mateconf/201930403002>
18. A. Zinkovskii, K. Savchenko, and Ya. Kruglii, “Influence of modeling of contact interaction conditions on spectrum of natural vibration frequencies of blade assembly,” in: K. Vogiatzis, G. Kouroussis, M. Crocker, and M. Pawelczyk (Eds.), *From Ancient to Modern Acoustics: 23rd Int. Congress on Sound and Vibration 2016 (ICSV 23)* (July 10–14, 2016, Athens, Greece), Vol. 1 (2016), pp. 289–293.
19. M. P. Castanier and C. Pierre, “Modeling and analysis of mistuned bladed disk vibration: status and emerging directions,” *J. Propul. Power*, **22**, No 2, 384–396 (2006).
20. Yu. S. Vorob’ev, *Vibration of the Blade Outfit of Turbomachines* [in Russian], Naukova Dumka, Kiev (1988).